entropy

MDPI

Article

Quantum-Walk-Inspired Dynamic Adiabatic Local Search

Chen-Fu Chiang [1,*] and Paul M. Alsing [2]

[1] Department of Computer Science, State University of New York Polytechnic Institute, Utica, NY 13203, USA
[2] Information Directorate, Air Force Research Laboratory, Rome, NY 13441, USA; paul.alsing@us.af.mil
* Correspondence: chiangc@sunypoly.edu

Abstract: We investigate the irreconcilability issue that arises when translating the search algorithm from the Continuous Time Quantum Walk (CTQW) framework to the Adiabatic Quantum Computing (AQC) framework. For the AQC formulation to evolve along the same path as the CTQW, it requires a constant energy gap in the Hamiltonian throughout the AQC schedule. To resolve the constant gap issue, we modify the CTQW-inspired AQC catalyst Hamiltonian from an XZ operator to a Z oracle operator. Through simulation, we demonstrate that the total running time for the proposed approach for AQC with the modified catalyst Hamiltonian remains optimal as CTQW. Inspired by this solution, we further investigate adaptive scheduling for the catalyst Hamiltonian and its coefficient function in the adiabatic path of Grover-inspired AQC to improve the adiabatic local search.

Keywords: quantum walk; adiabatic quantum computing; adiabatic path scheduling; catalyst Hamiltonian

Citation: Chiang, C.-F.; Alsing, P.M. Quantum-Walk-Inspired Dynamic Adiabatic Local Search. *Entropy* **2023**, *25*, 1287. https://doi.org/10.3390/e25091287

Academic Editors: Giuliano Benenti and Brian R. La Cour

Received: 10 August 2023
Accepted: 27 August 2023
Published: 31 August 2023

1. Introduction

Quantum technologies have advanced dramatically in the past decade, both theoretically and experimentally. From the view of theoretical computational complexity, Shor's factoring algorithm [1] and Grover's search algorithm [2] are well-known for their improvements over the best possible classical algorithms designed for the same purpose. From a perspective of universal computational models, Quantum Walks (QWs) have become a prominent model of quantum computation due to their direct relationship to the physics of the quantum system [3,4]. It has been shown that the QW computational framework is universal for quantum computation [5,6], and many algorithms now are presented directly in the quantum walk formulation rather than through a circuit model or other abstracted method [3,7]. Besides being search algorithms, CTQWs have been applied in fields such as quantum transport [8–11], state transfer [12,13], link prediction in complex networks [14] and the creation of Bell pairs in a random network [15]. Some other well known universal models include the quantum circuit model [16–18], topological quantum computation [19], adiabatic quantum computation (AQC) [20], resonant transition-based quantum computation [21] and measurement-based quantum computation [22–25]. Investigating relationships among the frameworks helps to identify violations when mapping frameworks and potential solutions. By studying the mapping, one can extend the techniques from one framework to another for some potential improvement in terms of speed [26].

In this work, we investigate the irreconcilability issue that arises when translating the search algorithm from the Continuous Time Quantum Walk (CTQW) framework to the Adiabatic Quantum Computing (AQC) framework as first pointed out by Wong and Meyer [27]. This irreconcilability issue can be described as follows. One first notes that the CTQW is the unique continuous time quantum walk formulation of Grover's discrete search algorithm. While the CTQW search evolves the initial unbiased (equal amplitude) state to the unknown (marked) state on the order of time $T \sim \mathcal{O}(\sqrt{N})$ (where N is the size of the search space), it does not follow the same evolution path (on the Bloch sphere) as that of Grover's algorithm. The uniqueness of the CTQW formulation stems from the fact

that the unknown marked state only acquires a (time-dependent) phase from the oracle operation. Most importantly the marked states do not undergo evolution, and thus the CTQW effectively employs a dichotomous "Yes/No" oracle, for which the discrete Grover's algorithm has been proven to be optimal.

The AQC formulation of the search algorithm with a non-uniform adiabatic evolution schedule [28] also finds the marked state in time $T \sim \mathcal{O}(\sqrt{N})$ while following the same path as Grover's algorithm. Thus, if one investigates what adiabatic Hamiltonian gives rise to the same evolution path as the CTQW formulation, one finds [27] that the AQC formulation introduces an extra "catalyst" Hamiltonian which introduces a structure beyond the standard "Yes/No" oracle employed in the CTQW or discrete (Grover's) search algorithm. A scaled version of the AQC Hamiltonian leads to a constant energy gap that implies that the marked state can be found in time $T \sim \mathcal{O}(1)$. This discrepancy between the formulations of the two versions of a continuous time search algorithm was termed the "irreconcilability (difference) issue" between CTQW and AQC by Wong and Meyer [27].

In this work, we address the CTQW/AQC search algorithm irreconcilability issue by modifying the constant energy gap Hamiltonian of the AQC formulation. Our contribution is twofold. We first adapt the result from the mapping of CTQW to AQC by selecting the regular oracle Z operator as the catalyst Hamiltonian and explore an alternative for the coefficient function for the catalyst Hamiltonian in order to attempt to avoid the irreconcilability issue. Through the simulation, the modified model provides optimal results in terms of the time required for the search.

The second improvement is on the Grover-Search-inspired adiabatic local search, we add an additional sluggish parameter δ which delineates the width of the adiabatic run time schedule over which the catalyst Hamiltonian effectively acts (i.e., the "slowdown" region in the vicinity of the system's smallest energy gap Δ). The sluggish parameter tracks the increase of running time $t = t(s)$ with respect to schedule parameter $0 \leq s \leq 1$ where $\delta = |d^2t/ds^2|$. The catalyst is employed when $\delta \geq \delta_0$ to facilitate the process; we have found that the threshold value of $\delta_0 = 64$ provides good results. When simulated, this modification reduces the running time of the original adiabatic local search by certain constant factors.

The outline of this work is as follows. The background information regarding CTQW and AQC is given in Section 2 where the translation of CTQW to AQC is described in Section 3. The irreconcilability issue that occurs during the translation is explained in Section 3.1 and our proposed solution is provided in Section 3.2. The mapping of Grover search to AQC as an adiabatic local search is summarized in Section 4. We propose and describe the catalyst Hamiltonian mechanism in Section 4.1.2 and determine the sluggish interval where it is employed. We further explore three coefficient functions of the catalyst Hamiltonian in Section 4.1.3. The simulation results for the proposed modifications are discussed in Section 5. Finally, our conclusions are given in Section 6.

2. Background

2.1. Continuous Time Quantum Walk

Given a graph $G = (V, E)$, where V is the set of vertices and E is the set of edges, the CTQW on G is defined as follows. Let A be the adjacency matrix of G, the $|V| \times |V|$ matrix is defined component-wise as

$$A_{ij} = \begin{cases} 1 & \text{if } (i,j) \in E, \\ 0 & \text{otherwise} \end{cases} \tag{1}$$

where $i, j \in V$. A CTQW starts with a uniform superposition state $|\psi_0\rangle$ in the space, spanned by nodes in V, and evolves according to the Schrödinger equation with Hamiltonian A. After time t, the output state is thus

$$|\psi_t\rangle = e^{-iAt}|\psi_0\rangle. \tag{2}$$

The probability that the walker is in the state $|\tau\rangle$ at time t is given by $|\langle\tau|e^{-iAt}|\psi_0\rangle|^2$. To find the marked node $|\omega\rangle$ starting from an initial state $|\psi_0\rangle$ via a CTQW, one has to maximize the success probability

$$|\langle\omega|e^{-iAt}|\psi_0\rangle|^2 \tag{3}$$

while minimizing the time t. For instance, initially at time $t = 0$, the success probability is

$$|\langle\omega|e^{-iA0}|\psi_0\rangle|^2 = O(\frac{1}{|V|}). \tag{4}$$

The success probability is extremely small when the search space $|V| = N$ is large and $|\psi_0\rangle$ is a uniform superposition state.

When applied to spatial search, the purpose of a CTQW is to find a marker basis state $|\omega\rangle$ [29,30]. For this purpose, the CTQW starts with the initial state $|\psi_0\rangle = \sum_{i=1}^{N} \frac{1}{\sqrt{N}}|i\rangle$, and evolves according to the Hamiltonian [31]

$$H = -\gamma A - |\omega\rangle\langle\omega| \tag{5}$$

where γ is the coupling factor between connected nodes. The value of γ has to be determined based on the graph structure such that the quadratic speedup of CTQW can be preserved. Interested readers can refer to [29,31] for more details.

2.2. Adiabatic Quantum Computing

In the AQC model, H_0 is the initial Hamiltonian, H_f is the final Hamiltonian. The evolution path for the time-dependent Hamiltonian is

$$H(s) = (1 - s)H_0 + sH_f \tag{6}$$

where $0 \leq s \leq 1$ is a schedule function of time t. For convenience, we denote s as $s(t)$ and use them interchangeably. The variable s increases slowly enough that the initial ground state evolves and remains as the instantaneous ground state of the system. More specifically,

$$H(s(t))|\lambda_{k,t}\rangle = \lambda_{k,t}|\lambda_{k,t}\rangle \tag{7}$$

where $\lambda_{k,t}$ is the corresponding eigenvalue the eigenstate $|\lambda_{k,t}\rangle$ at time t and k labels for the k_{th} excited eigenstate. The minimal eigenvalue gap is defined as

$$g_{min} = \min_{0 \leq t \leq Ta} (\lambda_{1,t} - \lambda_{0,t}) \tag{8}$$

where T_a is the total evolution time of the AQC. Let $|\psi(T_a)\rangle$ be the state of the system at time T_a evolving under the Hamiltonian $H(s(t))$ from the ground state $|\lambda_{0,0}\rangle$ at time $t = 0$. The Adiabatic theorem [32,33] states that the final state $|\psi(T_a)\rangle$ is ϵ-close to the real ground state $|\lambda_{0,T_a}\rangle$ as

$$|\langle\lambda_{0,T_a}|\psi(T_a)\rangle|^2 \leq 1 - \epsilon^2, \tag{9}$$

provided that

$$\frac{|\langle\lambda_{1,t}|\frac{dH}{dt}|\lambda_{0,t}\rangle|}{g_{min}^2} \leq \epsilon. \tag{10}$$

There are several variations of AQC to improve the performance. The variations are based on modifying the initial Hamiltonian and the final Hamiltonian [34,35] or adding a catalyst Hamiltonian H_e [34], which is turned on/off at the beginning/end of the adiabatic

evolution. In this work, we are interested in the catalyst approach. A conventional catalyst Hamiltonian-assisted AQC path is expressed as

$$H(s) = (1-s)H_0 + s(1-s)H_e + sH_f. \tag{11}$$

3. Continuous Time Quantum Walk to Adiabatic Search Mapping

One can construct a time-dependent AQC Hamiltonian $H(s)$ as shown in [27] where the adiabatic search follows the CTQW search on a complete graph with N vertices. Let us define the following variables. The coupling factor γ is set to $1/N$ and $|\psi_0\rangle$ is the uniform superposition of all states in the search space. State $|r\rangle$ is the uniform superposition of non-solution states, state $|\omega\rangle$ is the solution state. Treating the state evolving in the CTQW system as the time-dependent ground state of $H(s)$, one constructs $H(s)$ in the $\{|\omega\rangle, |r\rangle\}$ basis as [27]

$$H(s) = \sqrt[4]{\frac{s(1-s)}{4\epsilon^2 N}}[(1-s)H_0 + \sqrt{s(1-s)}H_e + sH_f] \tag{12}$$

where $s(t) = sin^2(\frac{t}{\sqrt{N}})$ with

$$\begin{aligned} H_0 &= \left|\psi_0^{\perp}\right\rangle\left\langle\psi_0^{\perp}\right| - |\psi_0\rangle\langle\psi_0|, \quad H_f = |\gamma\rangle\langle\gamma| - |\omega\rangle\langle\omega|, \\ H_e &= 2i\sqrt{\frac{N-1}{N}}(|r\rangle\langle\omega| - |\omega\rangle\langle r|), \end{aligned} \tag{13}$$

or explicitily in the $\{|w\rangle, |r\rangle\}$ basis as

$$\begin{aligned} H_0 &= \begin{pmatrix} \frac{N-2}{N} & -2\frac{\sqrt{N-1}}{N} \\ -2\frac{\sqrt{N-1}}{N} & -\frac{N-2}{N} \end{pmatrix}, \\ H_e &= \begin{pmatrix} 0 & -2i\sqrt{\frac{N-1}{N}} \\ 2i\sqrt{\frac{N-1}{N}} & 0 \end{pmatrix}, \; H_f = \begin{pmatrix} -1 & 0 \\ 0 & 1 \end{pmatrix}. \end{aligned} \tag{14}$$

3.1. The Irreconcilability Issue: Constant Gap Catalyst Hamiltonian and Small Norm

The main concerns that are raised from Equation (12) are twofold. The first issue is the factor $\sqrt[4]{\frac{s(1-s)}{4\epsilon^2 N}}$ of $H(s)$. The adiabatic theorem [36] states that the system achieves a fidelity of $1-\epsilon$ to the target state, provided that

$$\frac{|\langle\frac{dH}{dt}\rangle_{0,1}|}{g_{min}^2} \leq \epsilon, \text{ where } g_{min} = \min_{0\leq t\leq T} E_1(t) - E_0(t). \tag{15}$$

Here, $\langle\frac{dH}{dt}\rangle_{0,1}$ are the matrix elements of dH/dt between the two corresponding eigenstates. $E_0(t)$ and $E_1(t)$ are the ground energy and the first excited energy of the system at time t. Given the $H(s)$ in Equation (12), one might conclude that a factor of $O(\sqrt[4]{1/N})$ significantly reduces the time required to achieve $1-\epsilon$ precision. This might be misleading as the g_{min} of $H(s)$ also carries the same factor. The second issue is that the catalyst H_e provides power greater than a typical Yes/No oracle as it maps non-solution states to a solution state and a solution state to non-solution states. Provided that we initially start with a superposition state with an amplitude of $\sqrt{\frac{N-1}{N}}$ for a non-solution, it takes a time of $O(1)$ for this catalyst to drive the initial (unbiased, equal amplitude) state to the solution state. In the following, we will relax this constraint by using a normal oracle. For the rest of the paper, let us simply treat $\epsilon \ll 1$ as a small negligible constant.

3.2. Modified CTQW-Inspired Adiabatic Search

In Equation (12), the following parameters were computed during the mapping [27]:

- the scaling factor $\sqrt[4]{\frac{s(1-s)}{4\epsilon^2 N}}$ of Hamiltonian H_0,
- $H_e = 2i\sqrt{\frac{N-1}{N}}(|r\rangle\langle\omega| - |\omega\rangle\langle r|)$, catalyst Hamiltonian
- the coefficient function of H_e as $\sqrt{s(1-s)}$.

In [37], the cost of the adiabatic algorithm was defined to be the dimensionless quantity (using $\hbar = 1$)

$$cost = t_f \max_s ||H(s)||, \tag{16}$$

where t_f is the running time. To prevent the cost from being manipulated to be arbitrarily small by changing the time units or distorting the scaling of the algorithm by multiplying the Hamiltonians by some size-dependent factor as shown in the irreconcilability concern [27], the norm of $H(s)$ should be fixed to some constant, such as 1.

To address the irreconcilability issue, the scaling factor is dropped and the catalyst Hamiltonian H_e is modified. Since $H_e = 2\sqrt{\frac{N-1}{N}}iXZ$ in the $\{|\omega\rangle, |r\rangle\}$ basis provides more power than a standard oracle, for our modification we remove the imaginary number i and the X operator. The operator Z alone behaves as a conventional "Yes /No" oracle in the $\{|\omega\rangle, |r\rangle\}$ basis. Let $M = 2\sqrt{\frac{N-1}{N}}$ and choose the modified adiabatic path $H_m(s)$ as

$$H_m(s) = (1-s)H_0 + f_z(s)MZ + sH_f, \tag{17}$$

where $f_z(s)$ is our chosen s-dependent coefficient for catalyst Z. In addition to $f_z(s) = \sqrt{s(1-s)}$ that was used in [27], functions that reach their maximum when $s = 1/2$ are good candidates for $f_z(s)$, such as $f_z(s) = \frac{\sin(s\pi)}{2}$. The use of the factor $1/2$ on the sine function is to offset the magnitude M to bound the norm of H_e as described in Equation (16).

4. Grover Search to Adiabatic Local Search Mapping

In this section we consider the mapping of Grover's algorithm to an adiabatic search. Given the initial driving Hamiltonian H_0 and the final Hamiltonian H_f as

$$H_0 = I - |\psi_0\rangle\langle\psi_0|, \quad H_f = I - |\omega\rangle\langle\omega|, \tag{18}$$

where

$$H_0 = \begin{pmatrix} \frac{N-1}{N} & -\frac{\sqrt{N-1}}{N} \\ -\frac{\sqrt{N-1}}{N} & \frac{1}{N} \end{pmatrix}, H_f = \begin{pmatrix} 0 & 0 \\ 0 & 1 \end{pmatrix}, \tag{19}$$

in the $\{|\omega\rangle, |r\rangle\}$ basis. The adiabatic path [27,28] in the $\{|\omega\rangle, |r\rangle\}$ basis is given by

$$H(s) = (1-s)H_0 + sH_f \tag{20}$$

$$= \begin{pmatrix} (1-s)\frac{N-1}{N} & -(1-s)\frac{\sqrt{N-1}}{N} \\ -(1-s)\frac{\sqrt{N-1}}{N} & 1-(1-s)\frac{N-1}{N} \end{pmatrix}. \tag{21}$$

Instead of employing a linear evolution of $s(t)$, Equation (20) adapts the evolution ds/dt to the local adiabaticity condition [28] such that

$$|\frac{ds}{dt}| = \epsilon g^2(t) \tag{22}$$

where $g(t)$ is the energy gap of the system at time t. The running time t is then a function of schedule s such that

$$t(s) = \frac{N}{2\epsilon\sqrt{N-1}}\Big\{\arctan\Big(\sqrt{N-1}(2s-1)\Big) \tag{23}$$

$$+\arctan\Big(\sqrt{N-1}\Big)\Big\}. \tag{24}$$

The relationship between the schedule s and the running time t is shown in Figure 2 in [28]. It is a tailored schedule that goes fast in the outer regions and slows down near the gap. It is clear that the system evolves quickly when the gap is large (s away from $1/2$) and slowly when the gap is small ($s \simeq 1/2$) [28]. In this example, the sluggish period $s \in [0.4, 0.6]$. For completeness, we provide the formal proof of the close form of the squared gap function $g^2(t)$ (second order in s) with respect to the schedule s in Appendix A.

4.1. Adaptive Scheduling

For a fixed schedule of an adiabatic path, the schedule s moves fast when the eigen-energy gap is large, and slowly when the gap is small. We desire to employ the catalyst Hamiltonians H_e to amplify the eigen-energy gap during the "slow down" period such that the total time to pass through the sluggish period is reduced ($s \in [0.4, 0.6]$ in Figure 2 in [28].

4.1.1. Schedule-Dependent Gap Function

In this section, we consider employing gap-dependent scheduling functions. Let H_f be an arbitrary 2 by 2 Hermitian Hamiltonian. Let the time-dependent Hamiltonian $H(s)$ be

$$H(s) = (1-s)H_o + f_x(s)\sigma_x + f_z(s)\sigma_z + sH_f. \tag{25}$$

Operators σ_x and σ_z are chosen as catalyst Hamiltonians. Let $H_o = \begin{bmatrix} a & c \\ c & b \end{bmatrix}, H_f = \begin{bmatrix} p & r \\ r & q \end{bmatrix}$ where a, b, c, p, q, r are some given constants. The matrix form of the time-dependent Hamiltonian is given by

$$H(s) = \begin{bmatrix} (1-s)a + sp + f_z(s) & (1-s)c + sr + f_x(s) \\ (1-s)c + sr + f_x(s) & (1-s)b + sq - f_z(s) \end{bmatrix} \tag{26}$$

and the schedule-dependent gap can be analytically computed to yield

$$g^2(s) = ((1-s)(a-b) + s(p-q) + 2f_z(s))^2$$

$$+ 4((1-s)c + sr + f_x(s))^2, \tag{27}$$

(see Appendix B for a derivation). By using Equation (22), the total running time T^{stp}_{strt} from $s = s_{strt}$ to $s = s_{stp}$ is thus

$$T^{s_{stp}}_{s_{strt}} = \int_{s_{strt}}^{s_{stp}} \frac{ds}{\epsilon g^2(s)} \tag{28}$$

where $0 \le s_{strt} \le s_{stp} \le 1$. In brief, the time spent during a certain period of a schedule can be obtained by use of a gap function. The gap function can be expressed via the entries of H_0, H_e, H_f, schedule s and the coefficient functions of the catalyst Hamiltonians.

4.1.2. Determining the Sluggish Interval for the Catalyst Hamiltonian

By using the condition $f'(s) = dt/ds = \frac{1}{\epsilon g^2(s)}$ (see Appendix A), the region where the gap quickly significantly decreases or increases is during the sluggish period of s. That is the portion of the schedule s where a catalyst should be employed. The region where $|df^2(s)/ds^2)| \ge \delta_0$ is the sluggish period. The threshold value $\delta_0 = 64$ was chosen because

if we choose a threshold proportional to N, as N increases exponentially, the quantity d^2t/ds^2 might never reach the N-dependent threshold within the adiabatic evolution schedule $0 \leq s \leq 1$. By using this threshold, the starting point s^{slug}_{strt} and the stopping point s^{slug}_{stp} used to mark the sluggish period can be identified. Using the example in [28], we can re-plot and get t as a function of s as $t = f(s)$ and $f'(s) = dt/ds$ in Figures 1 and 2 with $N = 64$.

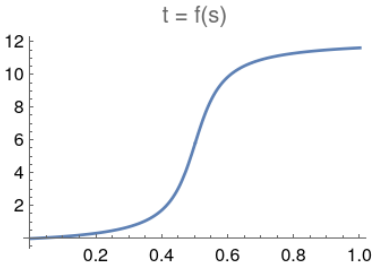

Figure 1. Time t as a function of schedule s for adiabatic local search with $N = 64$.

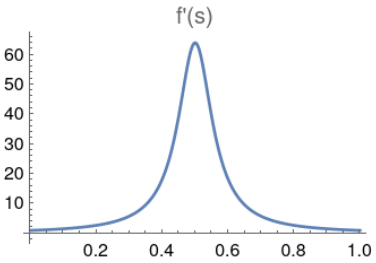

Figure 2. dt/ds for adiabatic local search with $N = 64$.

4.1.3. Catalyst Coefficient Functions

As discussed in Section 3.2, we are interested in the $H_e = Z$ case in Equation (17) and its coefficient function $f_z(s)$. Three coefficient functions of the catalyst Hamiltonian Z are proposed as the following

$$\begin{aligned} f_z^{sine}(s) &= \sin(((s - s^{slug}_{strt}) * \pi)/(s^{slug}_{stp} - s^{slug}_{strt})), \\ f_z^{ss}(s) &= (s - s^{slug}_{strt})(s^{slug}_{stp} - s), \\ f_z^{grid}(s) &= a * f_z^{sine}(s) + b * (f_z^{sine}(s))^2 \end{aligned} \tag{29}$$

where $0 \leq a, b \leq 1$ under the constraint that $a^2 + b^2 = 1$. In the grid search a increased from 0 to 1 by 0.1 in each iteration. From the 10 pairs of (a, b), we find the values of a, b that give the shortest sluggish time interval.

5. Experiment and Result

For our simulations we used (Wolfram) Mathematica (version 12.3 run on a Linux Ubuntu 20.04 LTS laptop). The code is available upon request. The running time is based on Equation (28). The size N (number of nodes) ranges from $2^5, 2^6, \ldots$ to 2^{25}. We observe the corresponding running time and sluggish time for each of the proposed models. The result of the original adiabatic local search serves as the baseline for comparison, which used $N = 64$ [28]. In this work, we generalize the setting for any arbitrary size N.

Given an arbitrary complete graph of size N with coupling factor $1/N$, one can compute the entries in the reduced Hamiltonian for H_0 and H_f in the $\{|\omega\rangle, |r\rangle\}$ basis. The values of variables a, b, c, p, q and r as discussed in Section 4.1.1 can be obtained from Equation (14) for the CTQW case and from Equation (19) for the adiabatic local search. It is worth noticing that the ground state energy is -1 in the CTQW case, but is 0 in the adiabatic local search case. Based on the adiabatic path Equation (25) and the gap function

in Equation (27) with given schedule s, coefficient function $f_z(s)$ for σ_z, we perform the simulation with the running time computed from Equation (28).

5.1. Modified CTQW-Inspired Adiabatic Search Simulation

This experiment aimed to demonstrate that the modified adiabatic paths addressing the irreconcilable issues remain optimal. The three proposed modifications we explored are as follows:

- $H_{org}(s)$ takes Equation (12) and drops the scaling factor as explained in Section 3.2. The adiabatic path is $H_{org}(s) = (1-s)H_0 + \sqrt{s(1-s)}H_e + sH_f$
- $H_{m1}(s)$ replaces the computed catalyst Hamiltonian H_e with an ordinary Z oracle operator and keeps the magnitude M. This was used to address the constant gap H_e irreconcilability issue. We have $H_{m1}(s) = (1-s)H_0 + \sqrt{s(1-s)}MZ + sH_f$
- $H_{m2}(s)$ uses $\frac{\sin(s\pi)}{2}$ as the coefficient function for the catalyst Hamiltonian Z. The adiabatic path is $H_{m2}(s) = (1-s)H_0 + \frac{\sin(s\pi)}{2}MZ + sH_f$

For the above three models, simulations were run on a Hamiltonian of size $N \in [2^5, 2^6, \ldots, 2^{25}]$. In the following figures, the abscissa is $\log_2 N$ while the ordinate is the required total running time T. The time is computed based on Equation (28). As the dimension of the Hamiltonian increases, the difference in running times for the three models considered are magnified.

The simulation results are shown in Figure 3. It is clear to see that H_{org} is a constant time scheme as it does not scale as the size N increases. This indicates that the original catalyst Hamiltonian $H_e = MXZ$ in $H_{org}(s)$ is indeed a constant gap Hamiltonian. This also shows the irreconcilability issue as suggested in [27]. From the simulations we can conclude that both $H_{m1}(s), H_{m2}(s)$ perform optimally with respect to running time, namely $T \sim \mathcal{O}(\sqrt{N})$, similar to that of the original adiabatic local search but with a minor constant factor which can be ignored in the Big O notation. As the simulation suggests, both modified CTQW-inspired approaches outperform the original adiabatic local search. When the $N \leq 2^{21}$, the $H_{m2}(s)$ outperforms $H_{m1}(s)$. When problem size N is larger then 2^{21}, $H_{m1}(s)$ is a better choice over $H_{m2}(s)$.

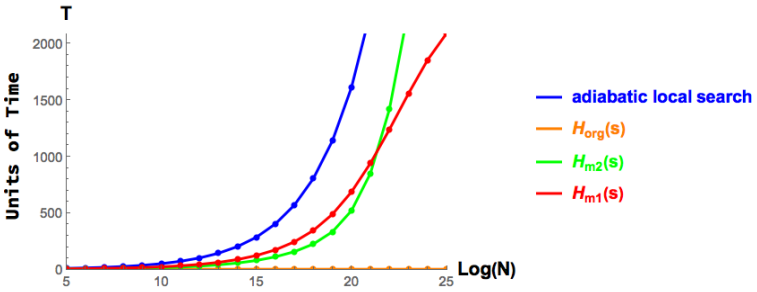

Figure 3. Case when $N \in [2^5, 2^{25}]$ and the running times of $H_{org}(s)$ (orange), $H_{m1}(s)$ (red) and $H_{m2}(s)$ (green) with the original adiabatic local search (blue) serving as the baseline.

5.2. Adaptive Adiabatic Local Search Simulation with Various Coefficient Functions

In the previous Section 5.1, the proposed modifications are optimal, in the sense that $T \sim \mathcal{O}(\sqrt{N})$ up to a minor constant factor. For further improvement, the adaptive scheduling scheme is applied. The adiabatic path to be explored is therefore

$$H_{adapt}(s) = (1-s)H_0 + f(s)Z + sH_f \tag{30}$$

where $f(s) \in [f_z^{sine}, f_z^{ss}, f_z^{grid}]$, as seen in Equation (29). The catalyst Hamiltonian Z operator is only employed during the sluggish period and hence $f(s) = 0$ when $s \notin [s_{strt}^{slug}, s_{stp}^{slug}]$. The

H_0 and H_f are based on Equation (19). As the catalyst is only employed within the sluggish period, to compare the performance of each proposed modification, one only needs to compute the running time within this period.

In Figure 4, f_z^{ss} provides the minimal reduced sluggish time while f_z^{sine} and f_z^{grid} provide significant improvements. The difference in the runtimes becomes significant for $N \geq 2^{15}$.

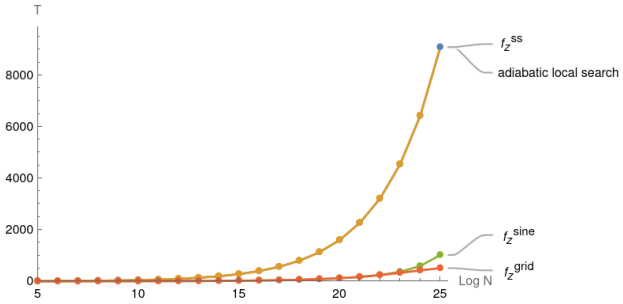

Figure 4. Case when $N \in [2^5, 2^{25}]$ and time spent in during the sluggish period for adiabatic paths with $(f_z^{ss}, f_z^{sine}, f_z^{grid})$ coefficient functions where the original adiabatic local search serves as the baseline.

In Figure 5, both f_z^{sine} and f_z^{grid} have a more than 75% reduced sluggish time in comparison to the original adiabatic local search when N reaches 2^{25}. f_z^{sine} gradually outperforms the original adiabatic local search after $N = 2^{10}$ and remains almost as good as f_z^{grid} until $N = 2^{23}$. When $N = 2^{25}$, the sluggish time of f_z^{sine} is only twice that of f_z^{grid}. In general, the grid search is a costly procedure as we have to run 10 pairs of (a, b) for slightly different $H(s)$ for each value of $N = 2^n$. If the time reduction of the sluggish period is not greater than 90% of the original, it might be a better choice to use f_z^{sine}. For the near term it might be more beneficial to use the f_z^{sine} model, instead of the grid search model f_z^{grid}.

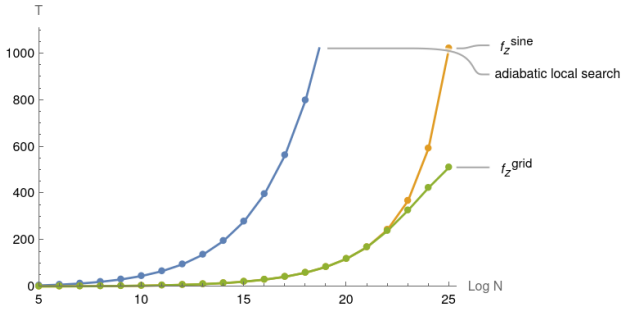

Figure 5. Case when $N \in [2^5, 2^{25}]$ and time spent during the sluggish period for adiabatic paths with (f_z^{sine}, f_z^{grid}) coefficient functions where the original adiabatic local search serves as the baseline.

6. Conclusions

In this work, we investigated different Hamiltonians for resolving the irreconcilability issue [27] when mapping the CTQW search algorithm to AQC. We modified the time-dependent Hamiltonian by (1) removing the original scaling CTQW factor $\sqrt[4]{\frac{s(1-s)}{4\epsilon^2 N}}$ and (2) replacing $i\,X\,Z \rightarrow Z$ in the original catalyst H_e Hamiltonian obtained from mapping CTQW to AQC. These modifications were made in order to resolve the irreconcilability issue. We further optimized the schedule s of the CTQW-inspired adiabatic path by an adaptive scheduling procedure.

The modified CTQW-inspired adiabatic search simulation experiment demonstrates that indeed the H_e without any modification leads to a constant time in the total running time, regardless of the search space size N. This result echoes the irreconcilability issue stated in [27]. On the other hand, the modified CTQW-inspired adiabatic path with catalyst Hamiltonian coefficient $\frac{\sin(s\pi)}{2}$ behaves similarly to the behavior of the optimal adiabatic

local search. Furthermore, the modifications are optimal and outperform the original adiabatic local search.

Lastly, in the adaptive adiabatic local search simulation with various coefficient functions experiment, we further investigated how to reduce the time wasted in the sluggish period of an adiabatic local search path. As our numerical experiments show, the function $f_z^{sine}(s)$ and $f_z^{grid}(s)$ provide significant improvement and both outperform the original adiabatic local search. Even though the grid search $f_z^{grid}(s)$ approach could have further reduced the length of the sluggish ("slow down") interval, the benefit was offset by the additional cost incurred from its implementation over that of the other two methods.

Author Contributions: Conceptualization, C.-F.C.; Methodology, C.-F.C. and P.M.A.; Validation, P.M.A.; Formal analysis, C.-F.C.; Investigation, C.-F.C. and P.M.A.; Writing—original draft, C.-F.C.; Writing—review & editing, P.M.A.; Supervision, P.M.A. All authors have read and agreed to the published version of the manuscript.

Funding: This research was funded by U.S. Air Force Research Lab Summer Faculty Fellowship Program (SFFP).

Institutional Review Board Statement: Not applicable.

Informed Consent Statement: Not applicable.

Data Availability Statement: The code for the simulation is available at https://github.com/omnibox/Quantum-Walk-Inspired-Dynamic-Adiabatic-Local-Search.

Acknowledgments: C.-F.C. gratefully acknowledges the support from the support from the Air Force Research Laboratory Summer Faculty Fellowship Program (SFFP). P.M.A. would like to acknowledge the support of this work from the Air Force Office of Scientific Research (AFOSR). Any opinions, findings and conclusions or recommendations expressed in this material are those of the author(s) and do not necessarily reflect the views of the Air Force Research Laboratory. The appearance of external hyperlinks does not constitute endorsement by the United States Department of Defense (DoD) of the linked websites, or the information, products or services contained therein. The DoD does not exercise any editorial, security or other control over the information you may find at these locations.

Conflicts of Interest: The authors declare no conflict of interest.

Appendix A. Time Integration of Adiabatic Local Search

Given a spectral gap polynomial of the second order, that is

$$g^2(s) = A(s^2 + bs + c) \tag{A1}$$

where s is the adiabatic schedule and (this is the same as $g^2(t)$ as for each t there is only one corresponding s) $\frac{ds}{dt} = \epsilon g^2(s)$, by integration on t one obtains

$$T = \int dt \quad = \quad \int_0^1 \frac{ds}{\epsilon g^2(s)} = \frac{1}{\epsilon A} \int_0^1 \frac{ds}{(s^2 + bs + c)}. \tag{A2}$$

(I) Case $b^2 - 4c > 0$: Let $r_\pm = \frac{-b \pm \sqrt{b^2-4c}}{2}$.

$$\int_0^1 \frac{ds}{(s^2 + bs + c)} = \frac{1}{r_+ - r_-} \int_0^1 (\frac{1}{s - r_+} - \frac{1}{s - r_-}) ds \tag{A3}$$

since $\int \frac{1}{s-a} ds = \ln|s - a|$. Thus, we have

$$T = \frac{1}{\epsilon A(r_+ - r_-)} \ln \left| \frac{s - r_+}{s - r_-} \right|_0^1, \tag{A4}$$

$$t = \frac{1}{\epsilon A(r_+ - r_-)} (\ln \left| \frac{s - r_+}{s - r_-} \right| - \ln \left| \frac{r_+}{r_-} \right|). \tag{A5}$$

(II) Case $b^2 - 4c = 0$:

$$\int_0^1 \frac{ds}{(s^2 + bs + c)} = \int_0^1 \frac{1}{(s + b/2)^2} ds \tag{A6}$$

since $\int (s-a)^{-2} ds = -(s-a)^{-1}$, hence

$$T = \frac{-1}{\epsilon A} \frac{1}{(s + (b/2))} \Big|_0^1 \tag{A7}$$

$$t = \frac{1}{\epsilon A} \Big(\frac{s}{(b/2)(s + (b/2))} \Big) \tag{A8}$$

(III) Case $b^2 - 4c < 0$:

$$\int_0^1 \frac{ds}{(s^2 + bs + c)} = \int_0^1 \frac{1}{(s + b/2)^2 + \frac{4c - b^2}{4}} ds \tag{A9}$$

$$= \int_{b/2}^{1+(b/2)} \frac{1}{x^2 + (\sqrt{\frac{4c-b^2}{4}})^2} dx \tag{A10}$$

since $\int \frac{1}{a^2 + x^2} dx = \frac{1}{a} \arctan \frac{x}{a}$. With $a = \sqrt{\frac{4c-b^2}{4}}$, we obtain

$$T = \frac{1}{\epsilon A} (\frac{1}{a}) (\arctan \frac{x}{a}) \Big|_{b/2}^{1+(b/2)} \tag{A11}$$

$$t = \frac{1}{\epsilon A} (\frac{1}{a}) (\arctan \frac{s + (b/2)}{a} - \arctan \frac{(b/2)}{a}) \tag{A12}$$

Appendix B. Energy Gap

Given an arbitrary 2 by 2 non-negative-entry Hermitian matrix H as

$$H = \begin{bmatrix} \alpha & \gamma \\ \gamma & \beta \end{bmatrix}, \tag{A13}$$

via computing the determinant and eigenvalues, the energy gap ΔE is

$$\Delta E = |\lambda_+ - \lambda_-| = \sqrt{(\alpha - \beta)^2 + 4\gamma^2}. \tag{A14}$$

Simply from the view of energy gap, as long as $|\gamma|$ increases and the gap, $|\alpha - \beta|$, between the diagonal entries increases, the energy gap would increase. The increase of $|\gamma|$ can be adapted by σ_x while $|\alpha - \beta|$ can be increased by σ_z. They should be good candidates for the catalyst perturbation in the AQC path. Similarly, if the Hamiltonian has an imaginary part in the off-diagonal entries,

$$H = \begin{bmatrix} \alpha & \gamma - di \\ \gamma + di & \beta \end{bmatrix} \tag{A15}$$

$$\Delta E = |\lambda_+ - \lambda_-| = \sqrt{(\alpha - \beta)^2 + 4(\gamma^2 + d^2)}. \tag{A16}$$

The Hamiltonian H (with no imaginery entries) can be expressed in terms of Pauli matrices as

$$H = \frac{\alpha+\beta}{2}\mathbb{I} + \frac{\Delta E}{2}((\frac{2\gamma}{\Delta E})\sigma_x + ((\frac{\alpha-\beta}{2})(\frac{2}{\Delta E})\sigma_z)) \tag{A17}$$

$$= \frac{\alpha+\beta}{2}\mathbb{I} + \frac{\Delta E}{2}A \tag{A18}$$

such that, by use of the power of Pauli matrices,

$$e^{-iHt} = \cos\left(\frac{\Delta E t}{2}\right)\mathbb{I} - i\sin\left(\frac{\Delta E t}{2}\right)A. \tag{A19}$$

References

1. Shor, P.W. Algorithms for quantum computation: Discrete logarithms and factoring. In Proceedings of the 35th Annual Symposium on Foundations of Computer Science, Santa Fe, NM, USA, 20–22 November 1994; pp. 124–134.
2. Grover, L.K. A fast quantum mechanical algorithm for database search. In Proceedings of the Twenty-Eighth Annual ACM Symposium on Theory of Computing, Philadelphia, PA, USA, 22–24 May 1996; pp. 212–219.
3. Farhi, E.; Gutmann, S. Quantum computation and decision trees. *Phys. Rev. A* **1998**, *58*, 915. [CrossRef]
4. Kempe, J. Quantum random walks: An introductory overview. *Contemp. Phys.* **2003**, *44*, 307–327. [CrossRef]
5. Childs, A.M. Universal computation by quantum walk. *Phys. Rev. Lett.* **2009**, *102*, 180501. [CrossRef] [PubMed]
6. Lovett, N.B.; Cooper, S.; Everitt, M.; Trevers, M.; Kendon, V. Universal quantum computation using the discrete-time quantum walk. *Phys. Rev. A* **2010**, *81*, 042330. [CrossRef]
7. Qiang, X.; Loke, T.; Montanaro, A.; Aungskunsiri, K.; Zhou, X.; O'Brien, J.L.; Wang, J.B.; Matthews, J.C. Efficient quantum walk on a quantum processor. *Nat. Commun.* **2016**, *7*, 1–6. [CrossRef] [PubMed]
8. Caruso, F.; Chin, A.W.; Datta, A.; Huelga, S.F.; Plenio, M.B. Highly efficient energy excitation transfer in light-harvesting complexes: The fundamental role of noise-assisted transport. *J. Chem. Phys.* **2009**, *131*, 09B612. [CrossRef]
9. Mohseni, M.; Rebentrost, P.; Lloyd, S.; Aspuru-Guzik, A. Environment-assisted quantum walks in photosynthetic energy transfer. *J. Chem. Phys.* **2008**, *129*, 11B603. [CrossRef] [PubMed]
10. Rebentrost, P.; Mohseni, M.; Kassal, I.; Lloyd, S.; Aspuru-Guzik, A. Environment-assisted quantum transport. *New J. Phys.* **2009**, *11*, 033003. [CrossRef]
11. Plenio, M.B.; Huelga, S.F. Dephasing-assisted transport: Quantum networks and biomolecules. *New J. Phys.* **2008**, *10*, 113019. [CrossRef]
12. Bose, S. Quantum communication through an unmodulated spin chain. *Phys. Rev. Lett.* **2003**, *91*, 207901. [CrossRef]
13. Kay, A. Perfect, efficient, state transfer and its application as a constructive tool. *Int. J. Quantum Inf.* **2010**, *8*, 641–676. [CrossRef]
14. Omar, Y.; Moutinho, J.; Melo, A.; Coutinho, B.; Kovacs, I.; Barabasi, A. Quantum Link Prediction in Complex Networks. *APS* **2019**, *2019*, R28-003.
15. Chakraborty, S.; Novo, L.; Ambainis, A.; Omar, Y. Spatial search by quantum walk is optimal for almost all graphs. *Phys. Rev. Lett.* **2016**, *116*, 100501. [CrossRef] [PubMed]
16. Shor, P.W. Quantum computing. *Doc. Math.* **1998**, *1*, 1.
17. Yao, A.C.C. Quantum circuit complexity. In Proceedings of the 1993 IEEE 34th Annual Foundations of Computer Science, Palo Alto, CA, USA, 3–5 November 1993; pp. 352–361.
18. Jordan, S.P.; Lee, K.S.; Preskill, J. Quantum algorithms for quantum field theories. *Science* **2012**, *336*, 1130–1133. [CrossRef] [PubMed]
19. Nayak, C.; Simon, S.H.; Stern, A.; Freedman, M.; Sarma, S.D. Non-Abelian anyons and topological quantum computation. *Rev. Mod. Phys.* **2008**, *80*, 1083. [CrossRef]
20. Mizel, A.; Lidar, D.A.; Mitchell, M. Simple proof of equivalence between adiabatic quantum computation and the circuit model. *Phys. Rev. Lett.* **2007**, *99*, 070502. [CrossRef] [PubMed]
21. Chiang, C.F.; Hsieh, C.Y. Resonant transition-based quantum computation. *Quantum Inf. Process.* **2017**, *16*, 120. [CrossRef]
22. Morimae, T.; Fujii, K. Blind topological measurement-based quantum computation. *Nat. Commun.* **2012**, *3*, 1036. [CrossRef]
23. Gross, D.; Eisert, J. Novel schemes for measurement-based quantum computation. *Phys. Rev. Lett.* **2007**, *98*, 220503. [CrossRef]
24. Briegel, H.J.; Browne, D.E.; Dür, W.; Raussendorf, R.; Van den Nest, M. Measurement-based quantum computation. *Nat. Phys.* **2009**, *5*, 19–26. [CrossRef]
25. Raussendorf, R.; Browne, D.E.; Briegel, H.J. Measurement-based quantum computation on cluster states. *Phys. Rev. A* **2003**, *68*, 022312. [CrossRef]
26. Cutugno, M.; Giani, A.; Alsing, P.M.; Wessing, L.; Schnore, S. Quantum Computing Approaches for Mission Covering Optimization. *Algorithms* **2022**, *15*, 224. [CrossRef]
27. Wong, T.G.; Meyer, D.A. Irreconcilable difference between quantum walks and adiabatic quantum computing. *Phys. Rev. A* **2016**, *93*, 062313. [CrossRef]

28. Roland, J.; Cerf, N.J. Quantum search by local adiabatic evolution. *Phys. Rev. A* **2002**, *65*, 042308. [CrossRef]
29. Childs, A.M.; Goldstone, J. Spatial search by quantum walk. *Phys. Rev. A* **2004**, *70*, 022314. [CrossRef]
30. Childs, A.M.; Cleve, R.; Deotto, E.; Farhi, E.; Gutmann, S.; Spielman, D.A. Exponential algorithmic speedup by a quantum walk. In Proceedings of the Thirty-Fifth Annual ACM Symposium on Theory of Computing, San Diego, CA, USA, 9–11 June 2003; pp. 59–68.
31. Novo, L.; Chakraborty, S.; Mohseni, M.; Neven, H.; Omar, Y. Systematic dimensionality reduction for quantum walks: Optimal spatial search and transport on non-regular graphs. *Sci. Rep.* **2015**, *5*, 13304. [CrossRef]
32. Farhi, E.; Goldstone, J.; Gutmann, S.; Sipser, M. Quantum computation by adiabatic evolution. *arXiv* **2000**, arXiv:quant-ph/0001106.
33. Albash, T.; Lidar, D.A. Adiabatic quantum computation. *Rev. Mod. Phys.* **2018**, *90*, 015002. [CrossRef]
34. Farhi, E.; Goldston, J.; Gosset, D.; Gutmann, S.; Meyer, H.B.; Shor, P. Quantum Adiabatic Algorithms, Small Gaps, and Different Paths. *Quantum Info. Comput.* **2011**, *11*, 181–214. [CrossRef]
35. Perdomo-Ortiz, A.; Venegas-Andraca, S.E.; Aspuru-Guzik, A. A study of heuristic guesses for adiabatic quantum computation. *Quantum Inf. Process.* **2011**, *10*, 33–52. [CrossRef]
36. Griffiths, D.J.; Schroeter, D.F. *Introduction to Quantum Mechanics*; Cambridge University Press: Cambridge, UK, 2018.
37. Aharonov, D.; Van Dam, W.; Kempe, J.; Landau, Z.; Lloyd, S.; Regev, O. Adiabatic quantum computation is equivalent to standard quantum computation. *SIAM Rev.* **2008**, *50*, 755–787. [CrossRef]